MAGNETIC FIELDS IN THE SOLAR CORONA

ANDREW C K LOW

Submitted in partial fulfilment of the requirements for the degree of Astrophysics
School of Physics and Astronomy
Queen Mary, University of London

ABSTRACT

This paper investigates magnetic fields in the solar corona. Magnetic fields undoubtedly play a dominant role in shaping the structure and dynamics of the corona. Understanding the magnetic fields is paramount in our quest to answer unanswered questions regarding the corona such as coronal heating. Unfortunately we are plagued with difficulties when observing the magnetic field on the corona. Only at the photospheric height can we easily observe magnetic fields made possible by the Zeeman effect, thus coronal magnetic fields must be extrapolated from the photosphere. Several different methods for this are explored, with a focus on the Green's function method. A numerical extrapolation of coronal magnetic fields is performed using the Green's function method. The magnetohydrodynamic equations are derived and their importance in solar and space plasma physics is discussed.

ACKNOWLEDGEMENTS

Dr. David Tsiklauri for continually outlining my lack of knowledge.
Poppy Green.
Paulo Ribeiro.
Jacob Pearce.

CONTENTS

LIST OF FIGURES

1

INTRODUCTION

The sun is our parent star, a giant sphere of bright burning plasma (an ionised gas considered the fourth state of matter). It is the source of most life and energy on Earth. As such it is no wonder that humans had once assigned mythological attributes to it. Some cultures even saw the sun as a deity, such as the ancient Egyptians who worshipped it as Ra and the Greeks who worshipped it as Helios (incidentally the etymological root of helium). As time passed, rigorous observations and the scientific method led to a refined comprehension of the sun. Copernicus correctly deducted that the sun is the centre of our solar system. Galileo's observations of sunspots led him to reason that the sun was a rotating sphere. A full understanding of the sun (i.e. the underlying processes that shape the structure and dynamics) has yet to be achieved even after many centuries of study. Humanity's ascent into space has allowed for improved observation of the sun with spacecrafts such as the Solar Dynamics Observatory (SDO), Solar Terrestrial Relations Observatory (STEREO) and Solar and Heliospheric Observatory (SOHO). These carry instruments which can collect data from beyond our visible spectrum; for example the Atmospheric Imaging Assembly (AIA) aboard the SDO and X-ray Telescope (XRT) aboard the Hinode photograph the sun in the Extreme Ultra Violet (EUV) and X-ray ranges respectively. Much of the electromagnetic radiation emitted by solar phenomena under study is in the invisible spectrum, thus these instruments provide us with clear details of interesting solar activity such as flares and coronal loops which would be difficult (but not impossible) to observe from Earth.

The sun consists of several distinct regions at different radii - the core, radiative zone, convective zone, photosphere, chromosphere, transition region and corona (the latter three are sometimes considered collectively as the solar atmosphere). The core is the hottest, densest part of the sun, with a temperature of around $15 \times 10^6 K$. Nuclear fusion occurs in the core producing helium from hydrogen mostly via the proton-proton chain reaction. The radiative and convective zones are responsible for the transport of energy generated from the nuclear core to the surface of the sun. Although both regions transport thermal energy, they do so using different processes which is reflected in their names.

The radiative zone extends from the core up to around 0.7 solar radii. In this region, thermal radiation transfers energy outwards from the core. Photons are emitted from hydrogen and helium ions and reabsorbed by other ions thus transferring energy. The convective zone lies above the radiative zone and extends to the solar surface. Similar to

the effect a heater has on air in a room, pockets of plasma are heated by the radiative zone below, lowering the density and causing them rise towards the surface. As they do so, heat is lost to the cooler plasma surrounding it. This increases the density of the plasma pocket and leads to it sinking back down towards the top of the radiative zone where it heats up again and continues the cycle of convection.

The photosphere is the visible surface of the sun. H^- ions are the primary reason the sun is opaque below photospheric height as they absorb photons easily. The density of H^- ions is much smaller here which reduces the opacity, allowing photons to pass through.

The solar corona is the inconspicuous outermost region of the solar atmosphere. It's density is 10^{-12} times the density of the photosphere and as a result it is significantly dimmer than the rest of the sun. Due to this, the corona cannot be observed from earth without use of a coronagraph or the occurrence of a total solar eclipse.

The corona is extremely hot with a temperature of over $10^6 K$. In contrast, the photosphere is only around $5800K$, much cooler than the corona. This temperature difference seems puzzling as the energy heating the corona cannot be delivered from below it by traditional thermal means. This would violate the second law of thermodynamics since the solar surface is cooler than the corona. How the corona is so much hotter than the solar surface is still one of the major unanswered questions concerning the corona. Due to the extreme temperatures, metals can become highly ionised. This led to the inaccurate attribution of a coronal spectral line at 5303Å to an hypothetical undiscovered element called coronium as spectral lines at this wavelength did not correspond to any known element and had never been seen in laboratory conditions on Earth[1]. The actual source of this spectral line is Fe XIV (an iron ion).

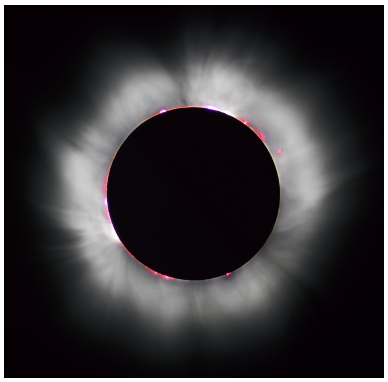

Figure 1: Solar corona made visible during a total eclipse in 1999.

Above the photosphere, a range of phenomena have been observed in 'active regions', such as sunspots, coronal loops, solar flares and coronal mass ejections, all of which are linked to magnetic activity in the sun. The quantity and frequency of these phenomena rise and fall periodically within what is known as a solar cycle (averaging 11 years per cycle). Sunspots, an iconic feature of the sun, are dark spots which appear on the photosphere and are a consequence of the differential rotation experienced by the sun. Since the

sun is plasma, the angular speed is not fixed like a solid. As a result we see a full rotation of the photosphere rotates every 25 whilst a full rotation at a latitude of 45^o needs 27.8 days[2]. Due to this differential rotation, magnetic field lines in the convective zone may become twisted and limit thermal convection to the photosphere at these points, manifesting as sunspots. As convection is limited at the sunspots, their temperature is lower than the neighbouring areas on the photosphere. Since the sun approximates a blackbody, its radiant emittance is proportional to the fourth power of temperature as given by the Stefan-Boltzmann Law: $j* = \sigma T^4$. Thus it is clear to see why sunspots appear darker than their surroundings (simply due to lower temperature). Sunspots usually come in pairs with opposite magnetic polarities. It has been shown that the active regions of the sun account for as much as 82.4% of the total required energy for coronal heating[3], thus we should study active regions in order to gain an understanding of the solar corona.

1.1 UNSOLVED PROBLEMS OF THE SOLAR CORONA

The most prominent problem regarding the corona is coronal heating. There are two main models that have been proposed to explain this phenomena - wave heating (DC) and current heating (AC). In the wave heating model, it is proposed that the solar interior produces various waves such as acoustic, gravitational and magnetohydrodynamic waves which dissipate in the corona releasing their energy[4]. However it has been shown that most waves do not reach the solar atmosphere, being reflected or damped due to shock formation. Alfvén waves are transverse in nature thus do not experience shock and damping, making them the most viable explanation for wave heating[5]. Alfvén waves are essentially oscillating ions within a plasma which do so due a restoring force given by the magnetic tension force $\frac{(B\cdot\nabla)B}{\mu_0}$ [6]. Alfvén waves are produced by the magnetic fields of the sun and the motion of plasma within it — since plasma is a conducting fluid, any movement (which could be due to rotation of the sun) gives the plasma an electromotive force which in turn produce waves.[7]. The fact that Alfvén waves do not dissipate before reaching the corona is also its downfall in explaining coronal heating, since they do not dissipate (and release energy) easily in the corona either.

The most popular hypothesis based on current heating relies on magnetic reconnection and nanoflares. Flares can be loosely defined as an observed brightening across any wavelength, with a lifespan in the order several minutes. Nanoflares are similar phenomena but happen must faster, with more than several thousand observed per second[8]. The active regions (typically regions above sunspots[1]) exhibit constantly shifting footpoints of

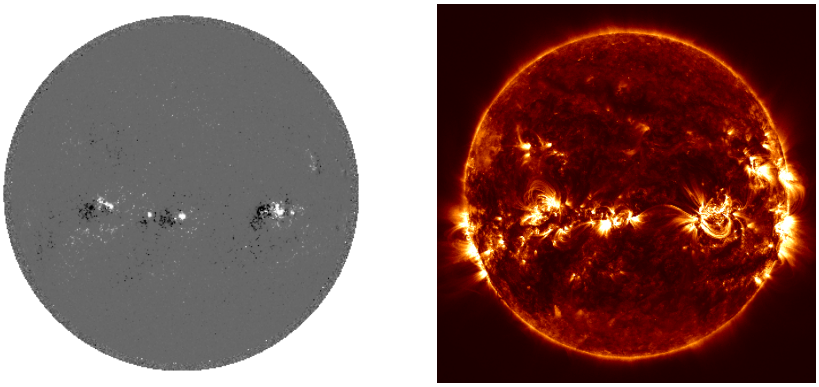

Figure 2: *Left*: HMI magnetogram (from 2nd of January 2014) showing line of sight value of normal magnetic field. Higher white value of pixel indicates higher magnitude of positive flux, and vice versa for black.
Right: Atmospheric Imaging Assembly image in the EUV wavelength range. Image shown was taken in the 171 Åwavelength. Coronal structures such as loops clearly visible.

the magnetic fields which occur due to convective motion below the photosphere[4]. This causes field lines to intertwine and knot together forming areas with high current known as current sheets or tangential discontinuities[9]. The tangential discontinuities build up and eventually dissipate and release energy as nanoflares via magnetic reconnection. This is where opposing magnetic field lines split and reconnect, releasing kinetic energy while doing so. This process however has been shown to be naturally too slow to cause flares, thus an "anomalous resistivity" is usually inserted to match observations.[10]

The solar corona is also subject to various observational problems. Unfortunately we can only reliably observe magnetic fields at photospheric height. Additionally many magnetograms only provide line-of-sight (longitudinal) values for magnetic field, B_l. Vector magnetograms provide values of transverse field components, however there exists a 180^o ambiguity in their direction.

EUV images such as the one shown in 2 visibly show us solar activity in the corona such as flares and coronal loops but give us no information about the properties of the magnetic fields in this domain. The influence of magnetic fields on the corona cannot be understated, consequently we see that this imperfect information is a great hindrance to understanding the corona. Since direct observation of the coronal magnetic fields with magnetograms is not possible, we must numerically extrapolate them from data provided with photospheric height magnetograms. This is discussed in detail in chapter 3.

2

THEORY OF CORONAL PLASMA PHYSICS

Let us construct a framework for mathematical descriptions of coronal plasma.

2.1 ELECTROMAGNETISM

Consider Maxwell's equations which provide a foundation for describing electromagnetism.

$$\nabla \cdot \mathbf{E} = \frac{\rho_q}{\epsilon_0} \tag{1}$$

$$\nabla \cdot \mathbf{B} = 0 \tag{2}$$

$$\nabla \times \mathbf{E} = -\frac{\partial \mathbf{B}}{\partial t} \tag{3}$$

$$\frac{1}{\mu_0} \nabla \times \mathbf{B} = \mathbf{j} + \epsilon_0 \frac{\partial \mathbf{E}}{\partial t} \tag{4}$$

where $\mathbf{E}$ is the electric field, $\mathbf{B}$ is the magnetic field, ρ_q is the charge density and $\mathbf{j}$ is the current density. Equation (4) can be simplified as we are within the context of non-relativistic plasma (the corona is plasma and $v \ll c$). Let us show that in the non-relativistic frame, the displacement current term, $\epsilon_0 {}^{\partial \mathbf{E}}/_{\partial t}$ can be neglected as it is much less than ${}^{1}/_{\mu_0} \nabla \times \mathbf{B}$.

Set L (where $L = \Delta x, \Delta y, \Delta z$)as the typical length scale of plasma inhomogeneity, so that any displacement of L will change the magnetic field by $B \approx \Delta B$. Set T as the typical time scale such that: ${}^{\partial}/_{\partial t} = {}^{1}/_{T}$ to estimate typical plasma speed, V. Thus we can approximate orders of magnitude for each variable in (4):

$$\frac{\partial \mathbf{B}}{\partial x} \approx \frac{\Delta B}{\Delta x} \approx \frac{B}{L} \qquad or \qquad \nabla \approx \frac{\partial}{\partial l} \approx \frac{1}{L}$$

$$V \approx {}^{L}/_{T}$$

Now we make use of Ohm's Law to examine the current density term. For a moving plasma, Ohm's Law is given by:

$$\mathbf{j} = \sigma(\mathbf{E} + \mathbf{v} \times \mathbf{B}) \tag{5}$$

where σ is conductivity. This is simply Ohm's Law for an immobile conductor, $\mathbf{j} = \sigma\mathbf{E}$, with the addition of a Lorentz force term, $\mathbf{F} = q(\mathbf{E} + \mathbf{v} \times \mathbf{B})$ due to magnetic influences. In fully ionized plasmas, conductivity is given by:

$$\sigma = \frac{n_e e^2}{\nu_e m_e} = \frac{n_e e^2}{m_e} \left(\frac{n_e e^4}{4\pi\epsilon_0^2 m_e^{0.5} k^{1.5} T^{1.5}} \right)^{-1}$$

$$= (2 \times 10^{-3}) T^{1.5}$$

We can see a proportional relationship exists between conductivity and temperature, namely $\sigma \propto T^{1.5}$. Due to this relationship and the extremely high temperature of plasmas, it is clear that their conductivity is also extremely high, essentially allowing them to be treated as superconductors. Since conductivity can be defined as $\sigma = {}^{l}/_{RA}$, and superconductors have no resistance, as $R \to 0$, $\sigma \to \infty$. Although conductivity does not have a finite limit, current density $\mathbf{j}$ must remain finite (infinite current density would require infinite charge or area). Looking back at equation 5 with this in mind, it is clear to see that $(\mathbf{E} + \mathbf{v} \times \mathbf{B}) \to 0$ to keep $\mathbf{j}$ finite. We can equivalently say that $\mathbf{E} = -\mathbf{v} \times \mathbf{B}$, so $E \approx VB$.

These order of magnitudes can used to estimate the ratio of the displacement current term, $\epsilon_0 {}^{\partial \mathbf{E}}/_{\partial t}$ and ${}^{1}/_{\mu_0}(\nabla \times \mathbf{B})$:

$$\epsilon_0 \frac{\partial \mathbf{E}}{\partial t} = \frac{\epsilon_0 E}{T} \qquad\qquad \frac{(\nabla \times \mathbf{B})}{\mu_0} = \frac{B}{L\mu_0}$$

$$\begin{aligned} ratio &= \frac{\epsilon_0 E}{T} \cdot \frac{L\mu_0}{B} \\ &= \epsilon_0 \mu_0 V^2 \\ &= \left(\frac{V}{C} \right)^2 \end{aligned}$$

Since we are in the non-relativistic frame, the ratio

$$({}^{V}/_{C})^2 \ll 1$$

i.e

$$\frac{\epsilon_0 \frac{\partial \mathbf{E}}{\partial t}}{\frac{1}{\mu_0}(\nabla \times \mathbf{B})} \ll 1$$

This shows that the displacement current is many orders of magnitude smaller allowing us to neglect it and rewrite equation (4) simply as:

$$\mathbf{j} = \frac{1}{\mu_0} \nabla \times \mathbf{B} \tag{6}$$

We can also use Ohm's Law to rewrite equation (3) in terms of only magnetic fields. Rearranging Ohm's Law in equation (5) to make **E** the focus gives us:

$$\mathbf{E} = \frac{\mathbf{j}}{\sigma} - (\mathbf{v} \times \mathbf{B})$$

This can then be inserted into equation (3):

$$-\frac{\partial \mathbf{B}}{\partial t} = \nabla \times \left[\frac{\mathbf{j}}{\sigma} - (\mathbf{v} \times \mathbf{B})\right]$$

Equation (6) gives us the current density **j** of a plasma which we can also substitute in, thus the equation becomes:

$$\begin{aligned} \frac{\partial \mathbf{B}}{\partial t} &= -\nabla \times \left[\frac{\nabla \times \mathbf{B}}{\sigma \mu_0} - (\mathbf{v} \times \mathbf{B})\right] \\ &= \nabla \times (\mathbf{v} \times \mathbf{B}) - (\mu_0 \sigma)^{-1} \nabla \times (\nabla \times \mathbf{B}) \end{aligned} \tag{7}$$

Notice that we have a $\nabla \times (\nabla \times \mathbf{B})$ term in our equation expressing the curl of the curl of the magnetic field. This is equivalent to the following vector identity

$$\nabla \times (\nabla \times \mathbf{A}) = \nabla(\nabla \cdot \mathbf{A}) - \nabla^2 \mathbf{A} \tag{8}$$

Equation 2 is a constraint stating $\nabla \cdot \mathbf{B} = 0$. This allows us to simplify $\nabla \times (\nabla \times \mathbf{B})$ to $\nabla^2 \mathbf{B}$.

We can prove this vector identity using the Levi-Civita symbol (and kronecker delta function). The Levi-Civita symbol is denoted by the letter ϵ and is written with indices Ã la Einstein notation. It essentially represents a sign which is based on the permutation of the indices. When any of the indices are equal, the Levi-Civita symbol is zero for example $\epsilon_{121} = 0$, in three dimensions, the Levi-Civita is given by ϵ_{ijk} where even permutations of the indices yield +1 and odd permutations yield -1:

$$\varepsilon_{ijk} = \begin{cases} 0 & \text{if } i = j \text{ or } i = k \text{ or } j = k, \\ +1 & \text{if } (i,j,k) = (1,2,3) \text{ or } (2,3,1) \text{ or } (3,1,2), \\ -1 & \text{if } (i,j,k) = (3,2,1) \text{ or } (2,1,3) \text{ or } (1,3,2), \end{cases}$$

Thus the cross product of two vectors **u** and **v** can be expressed using the Levi-Civita symbol

$$[\mathbf{u} \times \mathbf{v}]_i = \epsilon_{ijk} \mathbf{u}_j \mathbf{v}_k$$

so

FOR $i = 1$

$$\begin{aligned}[\mathbf{u} \times \mathbf{v}]_1 &= \epsilon_{123} u_2 v_3 + \epsilon_{132} u_3 v_2 + \text{terms that cancel to zero due to repeated index} \\ &= u_2 v_3 - u_3 v_2\end{aligned}$$

FOR $i = 2$

$$\begin{aligned}[\mathbf{u} \times \mathbf{v}]_2 &= \epsilon_{213} u_1 v_3 + \epsilon_{231} u_3 v_1 + 0 \\ &= -u_1 v_3 + u_3 v_1\end{aligned}$$

FOR $i = 3$

$$\begin{aligned}[\mathbf{u} \times \mathbf{v}]_3 &= \epsilon_{312} u_1 v_2 + \epsilon_{321} u_2 v_1 + 0 \\ &= u_1 v_2 - u_2 v_1\end{aligned}$$

Thus the resultant vector is:

$$[\mathbf{u} \times \mathbf{v}] = \begin{bmatrix} u_2 v_3 - u_3 v_2 \\ u_3 v_1 - u_1 v_3 \\ u_1 v_2 - u_2 v_1 \end{bmatrix} \tag{9}$$

Now let us express the cross product of a cross product $\mathbf{u} \times (\mathbf{v} \times \mathbf{w})$

$$\begin{aligned}[\mathbf{u} \times (\mathbf{v} \times \mathbf{w})]_i &= \epsilon_{ijk} u_j (\mathbf{v} \times \mathbf{w})_k \\ &= \epsilon_{ijk} u_j \epsilon_{klm} v_l w_m \\ &= \epsilon_{ijk} \epsilon_{klm} u_j v_l w_m \end{aligned} \tag{10}$$

Here we have two Levi-Civita symbols, the product of which can be written in terms of the Kronecker delta as follows:

$$\epsilon_{ijk} \epsilon_{klm} = \delta_{il} \delta_{jm} - \delta_{im} \delta_{jl}$$

The Kronecker delta, is similar to the Levi-Civita symbol in that it's value depends on its indices. When the indices are equal, the Kronecker delta is unity and when they differ, the Kronecker delta is zero i.e.

$$\delta_{ij} = \begin{cases} 1 & \text{if } i = j \\ 0 & \text{if } i \neq j, \end{cases}$$

Thus equation (10) can be written as:

$$\begin{aligned}[\mathbf{u}\times(\mathbf{v}\times\mathbf{w})]_i &= u_j v_l w_m(\delta_{il}\delta_{jm}-\delta_{im}\delta_{jl})\\ &= \delta_{il}\delta_{jm}u_j v_l w_m-\delta_{im}\delta_{jl}u_j v_l w_m\\ &= \delta_{il}v_l(\delta_{jm}u_j w_m)-\delta_{im}w_m(\delta_{jl}u_j v_l)\end{aligned} \tag{11}$$

Recall that the Kronecker delta function is only equal to one when the indices are repeated, and zero for all else, therefore

$$\begin{aligned}[\mathbf{u}\times(\mathbf{v}\times\mathbf{w})]_i &= \delta_{ii}v_i(\delta_{mm}u_m w_m)-\delta_{ii}w_i(\delta_{jj}u_j v_j)\\ &= v_i(u_m w_m)-w_i(u_j v_j)\end{aligned}$$

$$\mathbf{u}\times(\mathbf{v}\times\mathbf{w})=\mathbf{v}(\mathbf{u}\cdot\mathbf{w})-\mathbf{w}(\mathbf{u}\cdot\mathbf{v}) \tag{12}$$

Substituting in the del operator ∇ and magnetic field $\mathbf{B}$ we find

$$\begin{aligned}\nabla\times(\nabla\times\mathbf{B}) &= \nabla(\nabla\cdot\mathbf{B})-\mathbf{B}(\nabla\cdot\nabla)\\ &= \nabla(\nabla\cdot\mathbf{B})-\nabla^2\mathbf{B}\end{aligned}$$

which proves the vector identify in (8), hence (7) can indeed be reduced to

$$\frac{\partial\mathbf{B}}{\partial t}=\nabla\times(\mathbf{v}\times\mathbf{B})+(\mu_0\sigma)^{-1}\nabla^2\mathbf{B} \tag{13}$$

2.2 FLUID MOTION

Since the solar corona is composed of plasma, we should include the motion of plasma in our framework. Plasma motion can be approached in a micro (kinetic) or macroscopic (fluid) manner. In the microscopic approach, each particle is considered individually. The equation of motion for a charged particle can be obtained by combining Newton's Second Law, $F=ma=m\ddot{x}$, with Lorentz Law, $F=q(\mathbf{E}+\mathbf{v}\times\mathbf{B})$:

$$\ddot{x}=\frac{q}{m}(\mathbf{E}+\mathbf{v}\times\mathbf{B}) \tag{14}$$

This equation of motion and Maxwell's equations are solved for each charged particle in the plasma, usually on a scale of 10^8 particles. This is known as the particle-in-cell (PIC) method.

The macroscopic approach is generally more useful. In this case we treat the plasma as a collective fluid rather than looking at each particle within it, as fluid motion is macroscopic. An important property of fluids is continuity which means that when we refer to

a small element of fluid, it is still large compared to the microscopic scale. Thus we can label a fluid "particle" as an infinitesimally small volume element of the fluid which itself contains many particles.

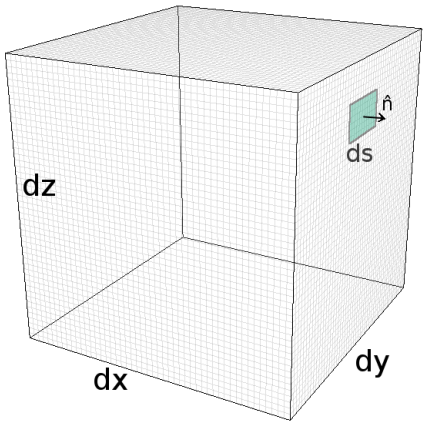

Figure 3: Volume element, dV, fixed in space with sides of length dx, dy, dz. A surface element with area ds with a normal unit vector, $\hat{n}$ is also shown. The surface element vector $(ds \cdot \hat{n})$is denoted as $d\mathbf{S}$

Figure 3 shows the volume element dV of a fluid. We will assume there are no sinks or sources in the volume element that will have an internal influence on the fluid flux. The size of dV is fixed, so the mass of fluid inside it at any time is given by:

$$M = \int \rho dV = \int p dx dy dx$$

where ρ is the density of $d\mathbf{S}$. The unit vector $\hat{n}$ is set to always point out of dV, so the direction of $d\mathbf{S}$ is always from the inside to outside. We can now define the outwards fluid flux through the element $d\mathbf{S}$ as:

$$\rho \mathbf{V} \cdot d\mathbf{S}$$

where $\mathbf{V}$ is the velocity vector of dV. The total outwards flux is therefore:

$$\oint p\mathbf{V} \cdot d\mathbf{S}$$

Due to the conservation of mass, this must be equal in magnitude (but opposite in sign) to the inwards flux. We can define the inwards flux as

$$-\frac{dM}{dt} = -\frac{d}{dt}\int \rho dV = -\int \frac{\partial \rho}{\partial t} dV$$

The conservation of mass can now be expressed as:

$$\oint \rho \mathbf{V} \cdot d\mathbf{S} + \int \frac{\partial \rho}{\partial t} dV = 0 \tag{15}$$

We can simplify this by applying Gauss' divergence theorem in order to change the closed surface integral into integral over the volume:

$$\int \nabla \cdot (\rho \mathbf{V}) dV + \int \frac{\partial \rho}{\partial t} dV = 0$$

$$\int \left(\nabla \cdot (\rho \mathbf{V}) + \frac{\partial \rho}{\partial t} \right) dV = 0 \tag{16}$$

In order for this expression to hold true for any volume regardless of shape or size, not just our volume element, we must conclude that

$$\nabla \cdot (\rho \mathbf{V}) + \frac{\partial \rho}{\partial t} = 0 \tag{17}$$

Now that we have obtained a mass conservation statement, we should express the equation of motion (conservation of momentum) for a plasma 'particle' analogous to the one for a charged particle shown in equation (14). Let's start with the definition of pressure - force per unit area:

$$p = \frac{F}{A} = \frac{dF}{dA}$$

thus each area element dA with a pressure of p experiences a force of dF. Applied to our fluid volume element dV, we can see that $dF = pd\mathbf{S}$ so the total force on dV is:

$$-\oint p d\mathbf{S} = -\int \nabla p dV$$

where we have once again used the divergence theorem to change the surface integral to volume integral. We can interpret this as the force per unit volume being $-\nabla p$, i.e. $\frac{F}{dV} = -\nabla p$. This can be combined with Newton's Second Law to obtain the equation of motion for a fluid volume element:

$$F = -\nabla p dV = ma = \rho dV \frac{d\mathbf{v}}{dt}$$

$$-\nabla p = \rho \frac{d\mathbf{v}}{dt} \tag{18}$$

As we are describing fluid, a continuous medium, the acceleration term $\frac{d\mathbf{v}}{dt}$ refers to the rate of change of velocity of a fluid element which is moving in space, rather than just the rate of change of velocity of the fluid at a fixed point in space. Thus in order to express this in fixed points quantities, we must recognise that the change in velocity $d\mathbf{v}$ (per time interval dt) is made up of two parts:

1. The change in velocity in the time interval dt at a fixed point in space given by the position vector $\mathbf{r}$.
$$\frac{\partial \mathbf{v}}{\partial t} dt$$
2. The difference in velocity of the fluid element at a fixed point in time of two points given by $\mathbf{r}$ and $\mathbf{r} + d\mathbf{r}$, where $d\mathbf{r}$ is the distance travelled in the time interval dt.
$$\frac{\partial \mathbf{v}}{\partial x} dx + \frac{\partial \mathbf{v}}{\partial y} dy + \frac{\partial \mathbf{v}}{\partial z} dz = (d\mathbf{r} \cdot \nabla)\mathbf{v}$$

so the change in velocity $d\mathbf{v}$ is given by:

$$d\mathbf{v} = \frac{\partial \mathbf{v}}{\partial t} dt + (d\mathbf{r} \cdot \nabla)\mathbf{v}$$

Thus the acceleration is:

$$\frac{d\mathbf{v}}{dt} = \frac{\partial \mathbf{v}}{\partial t} + (\mathbf{v} \cdot \nabla)\mathbf{v} \tag{19}$$

We can now substitute equation (19) into equation (18) to obtain the equation of motion for a *fluid*:

$$\rho \left(\frac{\partial \mathbf{v}}{\partial t} + (\mathbf{v} \cdot \nabla)\mathbf{v} \right) = -\nabla p \tag{20}$$

This equation does not take into account any external forces that act upon the fluid, thus is an incomplete description of plasma motion. Plasma consists of charged particles and as such, is able to carry current, thus to complete the equation of motion for *plasma* we must include electromagnetic influences. Assuming the plasma has a current density of $\mathbf{j}$, we know that it will experience a Lorentz force equal to $\mathbf{j} \times \mathbf{B}$. Thus our equation of motion can be corrected by simply adding this term to the existing force term, $-\nabla p$:

$$\rho \left(\frac{\partial \mathbf{v}}{\partial t} + (\mathbf{v} \cdot \nabla)\mathbf{v} \right) = \mathbf{j} \times \mathbf{B} - \nabla p \tag{21}$$

Recall that equation (6) defines the current density of plasma, so we can substitute this into equation (21) and complete our plasma motion equation:

$$\rho \left(\frac{\partial \mathbf{v}}{\partial t} + (\mathbf{v} \cdot \nabla)\mathbf{v} \right) = \frac{(\nabla \times \mathbf{B}) \times \mathbf{B}}{\mu_0} - \nabla p \tag{22}$$

2.3 MAGNETOHYDRODYNAMICS

We now have set of equations that describe the dynamics of motion and magnetic fields in plasma, namely equation (13), equation (17) and equation (22). As equations (22) and

(13) are vector equations, they technically represent three separate equations, one for each vector component (x,y,z). We therefore have seven equations, however there are eight variables - pressure p, density ρ, components of velocity vector v_x, v_y, v_z and components of magnetic field vector B_x, B_y, B_z, thus we must include an eighth equation, an equation of state:

$$p = p(\rho)$$

Hence our full set of equations is as follows:

$$\nabla \cdot (\rho \mathbf{V}) + \frac{\partial \rho}{\partial t} = 0 \tag{23}$$

$$\rho \left(\frac{\partial \mathbf{v}}{\partial t} + (\mathbf{v} \cdot \nabla)\mathbf{v} \right) = \frac{(\nabla \times \mathbf{B}) \times \mathbf{B}}{\mu_0} - \nabla p \tag{24}$$

$$\frac{\partial \mathbf{B}}{\partial t} = \nabla \times (\mathbf{v} \times \mathbf{B}) + (\mu_0 \sigma)^{-1} \nabla^2 \mathbf{B} \tag{25}$$

$$p = p(\rho) \tag{26}$$

This set of equations is called the Magnetohydrodynamics (MHD) equations; they describe the dynamics of magnetic fields in fluids that are electrically conductive. Note that in magnetohydrodynamics, we see no reference to electric forces. This is warranted as it can be seen that the electric force is negligible in non-relativistic plasmas (ratio of electric to magnetic forces is far less than one). Since 99% of all matter in the universe is composed of plasma, magnetohydrodynamics can be applied to a range of astrophysical systems. It also has applications on Earth where plasma plays a large role for example nuclear reactors.

3

METHODS FOR CALCULATING CORONAL MAGNETIC FIELDS

Understanding magnetic fields in the solar corona is important as they give us insight into the shape and dynamics of the corona. It has been shown that magnetic fields bear a large effect of the temperature structure and density of the corona. The hot and dense regions of the corona are associated with strong magnetic fields suggesting a link between coronal heating and solar magnetic fields.[11]

3.1 POTENTIAL FIELDS

Many forces can be described a as vector field. Some can be defined as the gradient of a scalar potential, and are called potential fields. Represented mathematically, we can say

$$F = \nabla\Phi$$

i.e. $F = \frac{d\Phi}{dx}\frac{d\Phi}{dy}\frac{d\Phi}{dz}$, where F is the potential field, Φ is the scalar potential and ∇ is the del operator representing the gradient. Commonly known fields of this nature are gravitational and electrostatic fields which have associated potential scalars.

Analogously we can describe a potential field for magnetism this way:

$$\mathbf{B} = \nabla\Phi$$

where **B** is the magnetic potential field and Φ is the magnetic scalar potential. Substituting this into equation (6)

$$\mathbf{j} = \mu_0(\nabla \times \nabla\Phi) = 0 \tag{27}$$

we can see that when we define **B** as a potential field, we must have current free assumption as the curl of a gradient is zero. We can prove this using equation (9) which we derived using the Levi-Civita symbol. We replace the vectors **u** and **v** respectively with

$$\nabla = \begin{bmatrix} \delta x \\ \delta y \\ \delta z \end{bmatrix} \qquad \textit{and} \qquad \nabla\Phi = \begin{bmatrix} \delta\Phi/\delta x \\ \delta\Phi/\delta y \\ \delta\Phi/\delta z \end{bmatrix}$$

$$
\begin{aligned}
[\nabla \times \nabla\Phi] &= \begin{bmatrix} \nabla_2\nabla\Phi_3 - \nabla_3\nabla\Phi_2 \\ \nabla_3\nabla\Phi_1 - \nabla_1\nabla\Phi_3 \\ \nabla_1\nabla\Phi_2 - \nabla_2\nabla\Phi_1 \end{bmatrix} \\
&= \begin{bmatrix} \delta^2\Phi/\delta y\delta z - \delta^2\Phi/\delta z\delta y \\ \delta^2\Phi/\delta z\delta x - \delta^2\Phi/\delta x\delta z \\ \delta^2\Phi/\delta x\delta y - \delta^2\Phi/\delta y\delta x \end{bmatrix} \\
&= \begin{bmatrix} 0 \\ 0 \\ 0 \end{bmatrix}
\end{aligned}
$$

Thus potential fields must be considered current free. This assumption of a current free corona/potential magnetic field seems misguided since the magnetic field should have a non-zero curl and therefore current if it is to deliver energy (magnetic fields are hypothesised to deliver energy to the corona and heat it). However coronal phenomena do seem to follow potential magnetic field lines.[12] For example, magnetic field lines of the corona are often traced out by coronal loops[13]. These loops usually have a semi-circular geometry spanning across two sunspots. Sunspots usually come in pairs of opposite magnetic polarity so as a simple approximation, we can model coronal loops with a magnetic dipole field. Here we outline such a procedure as shown in Aschwanden[14].

Consider a dipole in the centre of a spherical coordinate system (r, θ, φ). The components of the magnetic field due to current loop (in the region far from loop i.e. $r >> a$)are given as[25]:

$$B_r = (I\pi a^2)\frac{\mu_0}{2\pi}\frac{cos\theta}{r^3} \tag{28}$$

$$B_\theta = (I\pi a^2)\frac{\mu_0}{4\pi}\frac{sin\theta}{r^3} \tag{29}$$

$$B_\varphi = 0 \tag{30}$$

Let us now define the magnetic field as the gradient of a scalar function in spherical coordinates

$$\mathbf{B} = \nabla\Phi = \frac{\partial\Phi}{\partial r}\hat{\boldsymbol{r}} + \frac{1}{r}\frac{\partial\Phi}{\partial\theta}\hat{\boldsymbol{\theta}} + \frac{1}{r\sin\theta}\frac{\partial\Phi}{\partial\varphi}\hat{\boldsymbol{\varphi}}$$

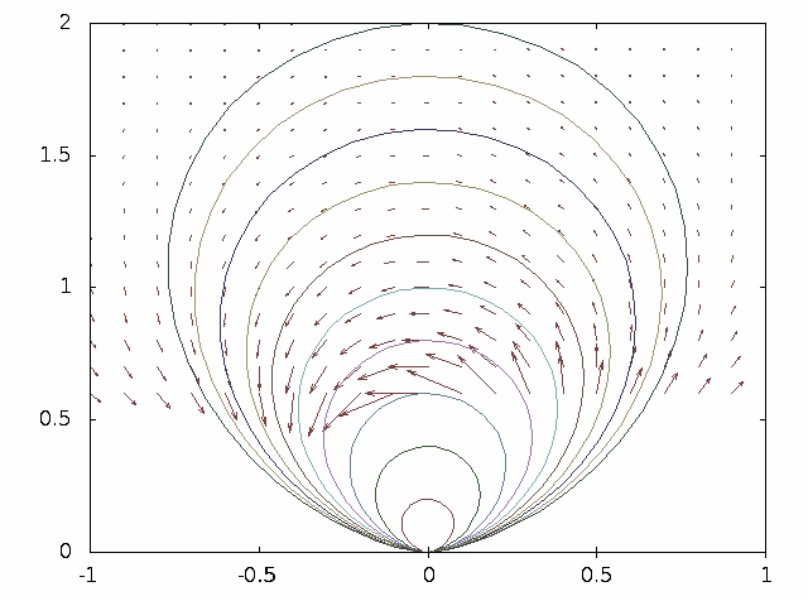

Figure 4: Dipole model of potential magnetic field.

Clearly our potential scalar function must be devoid of azimuthal, φ, terms as the azimuthal component of the magnetic field, B_φ, is zero thus we find that the scalar potential is

$$\Phi = \frac{-mcos\theta}{r^2}$$

We can now calculate the x and y components of the magnetic field which are given as[14]:

$$B_x = B_r cos\theta - B_\theta sin\theta$$

$$B_y = B_r sin\theta + B_\theta cos\theta$$

where B_r and B_θ are as given above and must be converted from polar to cartesian coordinates. Figure 4 shows an approximation of coronal loops with a dipole field in the (r, θ) plane. The x and y vector components of the potential field were calculated with the equations above and plotted as arrows. Field lines were plotted using the equation:

$$r = r_1 sin^2\theta$$

where r_1 is a constant which we set from 0.2 to 2 in increments of 0.2. The equation for r is derived from proportionality relations and a full derivation can be found in Aschwanden[14]. Here we take $y = 0.7$ as the photospheric height, and place the magnetic dipole below the solar surface at $y = 0$ such that the field threads through the surface. The field

lines do have a resemblance to coronal loops thus the potential field model can be seen as a viable approximation for the coronal magnetic field.

Let us apply this potential model to three dimensions as opposed to a two dimensional plane. Recall from equation (27) that we have a current free assumption allowing us to take the magnetic field as the gradient of a potential scalar, $\mathbf{B} = \nabla\Phi$. However the magnetic field must also be divergence free - a condition of Maxwell's equations (see equation (2)), therefore we can write this as:

$$\nabla \cdot \mathbf{B} = 0$$

$$\nabla \cdot \nabla\Phi = 0$$

$$\nabla^2\Phi = 0 \tag{31}$$

Equation (31) is known as Laplace's equation. This is a partial differential equation which we must solve to find the potential scalar function. If we choose to carry out our calculations using photospheric measurements near the centre of the solar disk, and on a region small enough that curvature is negligible, we can equate the line-of-sight magnetic field to the normal magnetic field on the boundary (i.e. photosphere), $B_l = B_n$. This is known as the classical Schmidt method as it was first done in this manner by Schmidt in 1964[15]. Let us define a coordinate system with the solar surface parallel to the (x, y) plane and the photospheric boundary as the $z = 0$ plane, with the z axis along the line-of-sight. With this coordinate system we can define the magnetic field measurement from magnetogram as the normal field component on the boundary, $B_n(x, y) = B_z(x, y, 0)$. The magnetic potential field in the volume above the boundary ($z > 0$) can be calculated from the scalar function. This scalar potential must satisfy Laplace's equation (31) and two boundary conditions. Since our line-of-sight magnetic field is the normal component of the derivative of the scalar function, $B_n = \frac{\delta\phi(r)}{\delta r_n}$, we can impose this as a lower boundary condition known as the Neumann boundary condition:

$$-\mathbf{n} \cdot \nabla\Phi = B_n \qquad (z = 0)$$

where $\mathbf{n}$ is the unit vector in the normal direction. The upper boundary condition simply ensures that the potential goes to 0 with large distance from origin:

$$\lim_{r\to\infty} \Phi(r) = 0 \qquad (z > 0)$$

Since we are solving a differential equation with boundary conditions, we can make use of the Green's function. Let's define an additional plane which lies on the $z = 0$ axis: $r' = (x', y', z) = (x', y', 0)$. This allows us to use a Green's function $G(r, r')$ to compute the

influence of the normal magnetic field component at each point on the r' (photosphere) plane on the magnetic potential field at $z > 0$[14]. The Green's function must satisfy several boundary conditions similar to those on the potential function, given as[16]:

$$-\mathbf{n} \cdot \nabla G(r, r') = 0 \qquad (z = 0)$$

$$\lim_{r-r' \to \infty} G(r, r') = 0 \qquad (z > 0)$$

$$\nabla^2 G(r, r') = 0 \qquad (z > 0)$$

It follows that the Green's function is:

$$G(r, r') = \frac{1}{2\pi R} = \frac{1}{2\pi |r - r'|} \tag{32}$$

Thus the scalar potential function can be found with an integration across the photospheric boundary plane r':

$$\begin{aligned} \Phi(r) &= \int B_n(r') G(r, r') dS' \\ &= \int \int B_n(r') G(r, r') dx' dy' \end{aligned}$$

where $B_n(r')$ is the normal magnetic field component, which we have equated to the line-of-sight field measurements. Note that the line-of-sight measurements are taken at points on a mesh at a distance of Δ apart, so each value is calculated from the average of the field in an area of Δ^2 around the point[16]. Thus it is more appropriate to use a summation rather than integral, replacing the variable of integration $dS' = dx'dy'$ with Δ^2:

$$\Phi(r) = \sum_{ij} B_n(r'_{ij}) G(r, r'_{ij}) \Delta^2 \tag{33}$$

This requires us to alter the boundary condition Neumann boundary condition to account for the mesh size[16]:

$$-\mathbf{n} \cdot \nabla G(r, r'_{ij}) = \begin{cases} 0 & (z = 0,\ |r - r'_{ij}| \gg \Delta) \\ 1/\Delta^2 & (z = 0,\ |r - r'_{ij}| \ll \Delta), \end{cases}$$

Thus our Green's function must also be altered to reflect this:

$$G(r, r') = \frac{1}{2\pi |r - r' + (\Delta/\sqrt{2\pi}) n|}$$

We can now insert this into equation (33) to calculate the scalar potential and potential field. Although this method is useful for approximation of magnetic fields in the corona, we must assume there is no current thus this model gives us no information about free energy available in electrical currents[17]. However many interesting phenomena such as solar flares and coronal mass ejections do contain current therefore the current free potential model is unsuitable for studying very active regions[18].

3.2 FORCE-FREE FIELDS

The simplest approach to allowing for electrical currents is the force-free model. This model assumes that the corona is not subject to any external non-magnetic forces. This is justified if we consider the ratio of magnetic pressure, $B^2/2\mu_0$, and plasma pressure, p, commonly known as β:

$$\beta = \frac{p}{B^2/2\mu_0} = \frac{2\mu_0 p}{B^2} \ll 1$$

We see that the ratio is far smaller than unity meaning plasma pressure is negligible when compared with magnetic pressure, thus we can ignore any non-magnetic forces on the coronal plasma[22]. We can therefore define force free fields to have no Lorentz force and write:

$$\mathbf{j} \times \mathbf{B} = 0 \tag{34}$$

Since the cross product of these two vectors is zero, we can see that the current density is parallel to magnetic field in a force-free field. we can rewrite this using a function, α, (known as the force-free or torsion function)

$$\mu_0 \mathbf{j} = \alpha \mathbf{B} \tag{35}$$

Recall that (6) gives us an equation for $\mu_0 \mathbf{j}$ which we can insert into equation (35) thus giving:

$$\nabla \times \mathbf{B} = \alpha \mathbf{B} \tag{36}$$

We can then take the divergence of (36) and use the vector identity $\nabla \cdot (\nabla \times \mathbf{u}) = 0$ to show:

$$\nabla \cdot (\nabla \times \mathbf{B}) = \nabla \cdot (\alpha \mathbf{B})$$
$$0 = \alpha(\nabla \cdot \mathbf{B}) + \mathbf{B} \cdot \nabla \alpha$$

We know from (2) that $\nabla \cdot \mathbf{B} = 0$ thus the above equation can be reduced to

$$\mathbf{B} \cdot \nabla \alpha = 0 \tag{37}$$

The α function represents a ratio of the current density and magnetic field strength[17].

3.2.1 *Linear force-free*

It is clear to see from (36) that the current free potential model discussed previously is just a special case of the force-free model where we set $\alpha = 0$. The next step up would be to assign α as a constant such that the condition posed in equation (37) is still met ($\nabla const = 0$). This is known as a linear force-free model as we have simplified the non-linear condition given in equation (36). Let us now take the curl of (36):

$$\begin{aligned} \nabla \times (\nabla \times \mathbf{B}) &= \nabla \times \alpha \mathbf{B} \\ &= \alpha(\nabla \times \mathbf{B}) \\ &= \alpha^2 \mathbf{B} \end{aligned} \tag{38}$$

Recall from equation (8) the vector identity $\nabla \times (\nabla \times \mathbf{A}) = \nabla(\nabla \cdot \mathbf{A}) - \nabla^2 \mathbf{A}$ which we proved with the Levi-Civita symbol. We can substitute this into equation (38) giving us

$$\nabla(\nabla \cdot \mathbf{B}) - \nabla^2 \mathbf{B} = \alpha^2 \mathbf{B}$$

We can again use the divergence free condition from equation (2) to reduce the above to

$$-\nabla^2 \mathbf{B} = \alpha^2 \mathbf{B}$$

$$\alpha^2 \mathbf{B} + \nabla^2 \mathbf{B} = 0 \tag{39}$$

Equation (39) is a form of the Helmholtz equation. Linear force-free fields can be calculated using only normal magnetic field components, B_n, making it a desirable simplification. Solutions for the linear force-free model have been achieved using a range of methods such as Green's function[19] [20] and Fourier series[21]. However, it has been shown that a constant α assumption is unrealistic within active solar regions thus we should set a changing α which is a function of position, i.e. $\alpha(r)$ [22].

3.2.2 *Non-linear force-free*

Using an α that is a function of position changes the model to a non-linear force-free one. In doing so, it is no longer possible to take only B_n as a boundary condition, thus we must include addition boundary conditions. This can be done by either stating the footpoints of the magnetic field lines, or by stating the value of α [27]. Recall that equation (37) restricts our choice of the α value by showing that there can be no change in α along a single magnetic field line, however different field lines can have different α values. Thus

we can see that the footpoints of each field line must be in positions where α is the same. The value of α at photospheric height (i.e. the z=0 plane) can be calculated with use of equation (36), when we have measurements for the tangential magnetic field components (these can be obtained from vector magnetograms), B_x and B_y, as well as the normal component:

$$\alpha = \left(\frac{\partial B_y}{\partial x} - \frac{\partial B_x}{\partial y} \right) \frac{1}{B_n} \tag{40}$$

Seeing as α should be the same at the two points of opposite polarity connected by a field line, the value is calculated for the area spanning just one of either the positive of negative magnetic polarity at the footpoint. This consequently averts a problem arising from measurement noise - if a field line with a footpoint at the point with the lowest α has the α at that point increased by noise, the condition in equation (36) no longer holds true[17]. Note that we can not only obtain an expression for α (40) from equation (36), but if we additionally make use equation (37) and (2) we can also obtain the derivatives with respect to the z axis for each magnetic field component and α. Furthermore these can all be expressed as functions of derivative in the x and y direction[14]:

$$\frac{\partial B_x}{\partial z} = \alpha B_y + \frac{\partial B_z}{\partial x}$$

$$\frac{\partial B_y}{\partial z} = -\alpha B_x + \frac{\partial B_z}{\partial y}$$

$$\frac{\partial B_z}{\partial z} = -\frac{\partial B_x}{\partial x} - \frac{\partial B_y}{\partial y}$$

$$\frac{\partial \alpha}{\partial z} = -\frac{1}{B_z} \left(B_x \frac{\partial \alpha}{\partial x} + B_y \frac{\partial \alpha}{\partial y} \right)$$

It is clear to see that by integrating the above differential equations with respect to z, the components of the magnetic field as well as α will be acquired for a step of dz. This can be done continually to obtain the coronal field to the desired height on the z axis. This method of extrapolating the coronal magnetic field is known as the upwards integration method. It is popular due to its relative simplicity in the context of computation. However, it is subject to various complications stemming from the fact that the above differential equations are based on an "ill-posed problem". Any inconsistencies in the boundary conditions, including measurement noise mentioned above, have a large effect on the solutions and have been shown to cause the extrapolated field to diverge[14][22]. This is clearly physically unrealistic as it is known that magnetic fields do not diverge ($\nabla \cdot \mathbf{B} = 0$).

Several other methods aside from upward integration also exist for calculating non-linear force-free models of the solar corona. The most widely used methods are: MHD

relaxation, Grad-Rubin iteration, boundary/Green's function and optimisation[23]. With the exponential increase of computational power available to the everyman in recent years, more complex models of the coronal field have been built and tested. Whereas exhaustive methods such as MHD relaxation would have needed supercomputers just a few decades ago due to the intensive computational requirements, the present day has perhaps allowed for such models to be run on personal computers[22]. The MHD relaxation method, as the name suggests makes uses of the MHD equations. Like a seed state for pseudorandom number generators, the current-free potential field is provided as a 'seed' to calculate the final force-free field. A Lorentz force is applied to photospheric height of the potential field to stress the field so that the tangential components of the magnetic field approximate those observed in vector magnetograms. The field is then 'relaxed' towards a equilibrium force-free state by balancing the Lorentz force with viscosity[28]. Here we outline the method for the case where the assumption $\beta = 0$ is made (known also as the magnetofrictional method). We start with a form of the equation of motion given in equation (24):

$$\rho\left(\frac{\partial \mathbf{v}}{\partial t} + (\mathbf{v}\cdot\nabla)\mathbf{v}\right) + \nabla p = \frac{(\nabla\times\mathbf{B})\times\mathbf{B}}{\mu_0} + \mathbf{D} \tag{41}$$

In order to 'relax' the field, the dissipative term which is a function of the velocity is also included in the equation of motion and is given as:

$$\mathbf{D} = -\nu\mathbf{v}$$

where ν is viscosity. It is this viscosity term that causes the dissipation function to relax the field. The viscosity term is usually artificially defined to speed up the relaxation to equilibrium. A common definition for the viscosity is given as:

$$\nu = \frac{\mathbf{B}^2}{\mu}$$

where μ is permeability and is taken as a constant. Thus we insert this into the dissipative term and rewrite it as:

$$\mathbf{D} = -\mathbf{v}\frac{\mathbf{B}^2}{\mu}$$

In this method the plasma beta is taken to be zero, i.e. only magnetic forces are relevant, all other external forces can be ignored. This allows us to completely ignore the terms on

the left hand side in equation (41) (note that the $-\nabla p$ term had already been moved to the LHS), thus we are left with:

$$\begin{aligned} 0 &= \frac{(\nabla \times \mathbf{B}) \times \mathbf{B}}{\mu_0} + \mathbf{D} \\ &= \frac{(\nabla \times \mathbf{B}) \times \mathbf{B}}{\mu_0} - \mathbf{v}\frac{\mathbf{B}^2}{\mu} \end{aligned}$$

Rearranging for the velocity we get:

$$\mathbf{v} = \frac{(\nabla \times \mathbf{B}) \times \mathbf{B}}{\mathbf{B}^2}$$

Recall from chapter 2.1 that in an ideal MHD system, we must have $\mathbf{E} = -\mathbf{v} \times \mathbf{B}$ in order to keep the current density finite. Notice that we can substitute the velocity expression above into $\mathbf{E}$:

$$\mathbf{E} = -\frac{((\nabla \times \mathbf{B}) \times \mathbf{B}) \times \mathbf{B}}{\mathbf{B}^2}$$

Finally we can use this definition of the electric field in Faraday's Law (or induction equation) given in equation (3) in order to obtain an expression for the rate of change of magnetic flux as it relaxes towards equilibrium:

$$\begin{aligned} \frac{\partial \mathbf{B}}{\partial t} &= -\nabla \times \mathbf{E} \\ &= \nabla \times \left[\frac{((\nabla \times \mathbf{B}) \times \mathbf{B}) \times \mathbf{B}}{\mathbf{B}^2} \right] \end{aligned} \tag{42}$$

Let us review the available extrapolation methods. The simplest model was the potential model. This was seen to be inadequate for modelling active regions due to current-free assumption. The linear-force free model was inadequate due to the constant alpha assumption. The non-linear force-free models currently provide the best description of coronal fields. Higher complexity models provide more accurate description of the coronal magnetic field, however require more observational data as input — potential field model only requires line-of-sight magnetograms, in contrast force-free models require vector magnetograms.

4

POTENTIAL FIELD CALCULATION USING GREEN'S FUNCTION

In this section we will apply the Green's function method to observed line of sight magnetic field components in a region near to the centre of the solar disc and small enough for curvature to be negligible. This is also known as the classical Schmidt method.

4.1 APPLICATION TO ARTIFICIAL DATA

Sunspots at the photospheric height are observed as the anchors at the end of coronal loops. These trace out the magnetic field lines which protrude out from the photosphere, thus we should expect to see similar loop like structures in our potential field model. Since sunspots come in pairs of opposite magnetic polarity, we could model a sunspot pair with the normal magnetic field given by two Gaussian functions of opposite sign:

$$B_n = A_1 \cdot \left[\frac{-(x-x_1)^2-(y-y_1)^2)}{\sigma_1^2}\right] - A_2 \cdot \left[\frac{-(x-x_2)^2-(y-y_2)^2)}{\sigma_2^2}\right] \tag{43}$$

where B_n is the normal magnetic field, a function of x and y. The sunspots are located at positions (x_1, y_1) and (x_2, y_2), with an amplitude of A_1 and A_2 respectively. The widths are denoted by σ_1 and σ_2. Figure 5 and 6 show a pair of sunspots we have modelled

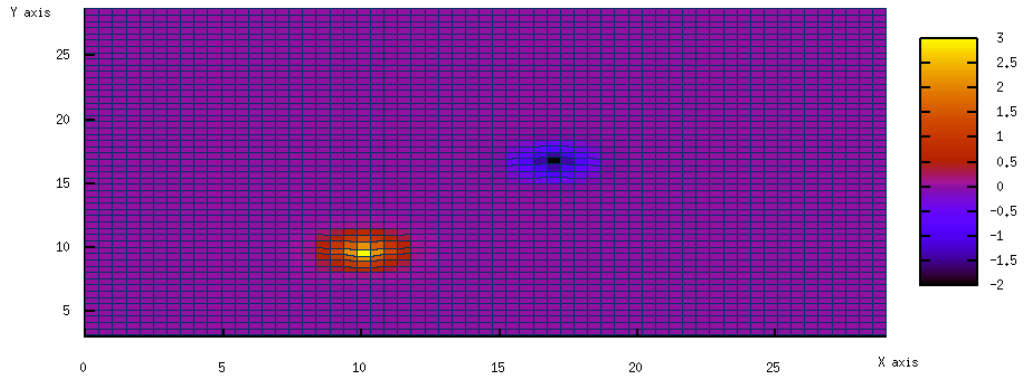

Figure 5: Plot of a sunspot pair modelled with a Gaussian function. Amplitude represented with a heat map.

using equation (43) to calculate the normal magnetic field component at each point. The

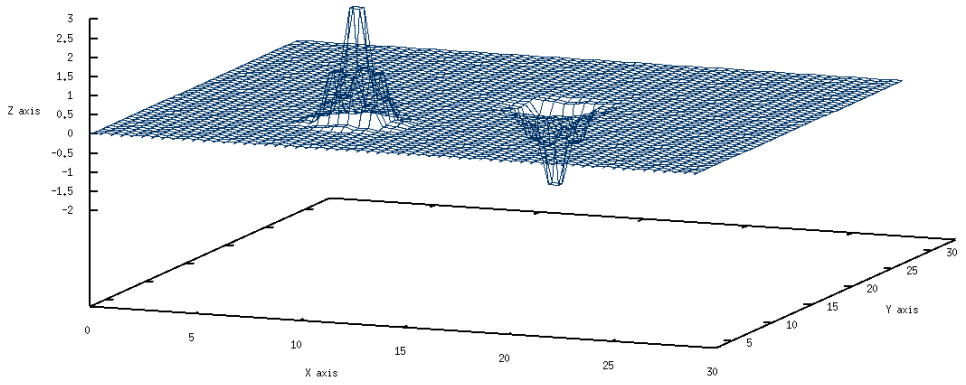

Figure 6: Plot of a sunspot pair modelled with a Gaussian function. Amplitude projected onto z axis for visual representation.

"sunspots" were placed at (10,10) and (17,17) — *i.e.* $(x_1, y_1) = (10, 10)$ *and* $(x_2, y_2) = (17, 17)$ within a box of side length 30 — with amplitudes of 3 and 2 respectively. The widths of both are set as $\sigma^2 = 1.2$. The artificial normal magnetic field values were computed and written to a file using python, which was then read into another program written to extrapolate the potential field using the Green's function method. This program is discussed in detail below, and the source code is available in the appendix of this document.

As we can see from figure 7 the potential field components computed from the artificial normal magnetic field components show loop like structures bearing a resemblance to coronal loops. Thus we see this model is viable for extrapolating potential fields and we can move forward to using observed data rather than artificial data.

4.2 APPLICATION TO OBSERVED DATA

The data used in our simulation was taken from the Helioseismic and Magnetic Imager (HMI), an instrument aboard the SDO that collects line-of-sight magnetograms among others. This was retrieved from the Joint Science Operations Center (JSOC) database.

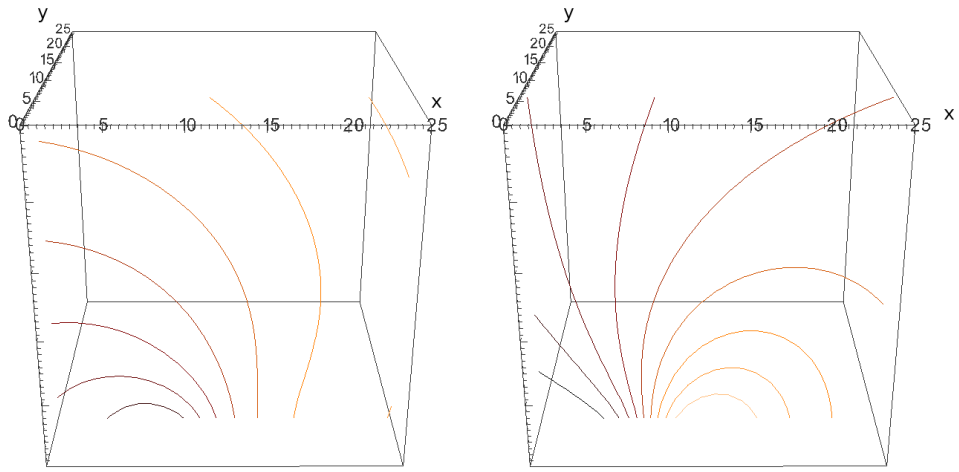

Figure 7: Plots showing a two dimensional contour slice of x and y components of the magnetic potential field calculated from artificial normal magnetic field data approximated with Gaussian function.

4.2.1 *Numerical setup*

The data from the HMI is given in the Flexible Image Transport System (.fits) file format, commonly used in scientific studies, especially in the astro fields. Each image has a size of 4096×4096 pixels. A program called fv, part of a larger software suite HEASOFT developed and maintained by NASA was used to extract data from the .fits file and convert it into a comma-separated values (.csv) format file. Each line of the .csv file corresponds to a line perpendicular to the y axis in our chosen region, with the line-of-sight magnetic field measurement for each point on the x axis contained within quotation marks and separated by commas. The .csv file is then fed into the main Java program which reads each line into an array with the `readData` method, then splits each value of the line by the comma with the `parseData` method, thus creating a two dimensional array (labelled as `data` in the code) containing the normal magnetic field values. This data is then used to calculate the potential Φ, given in equation (33). The potential is calculated for each position of x, y and z and stored in a three dimensional array (labelled as `phi` in the code). This is achieved by using the summation given in equation (33) within five nested loops,

one for each axis of r and r′ — i.e. x, y, z, x′ and y′. We take the mesh size to be unity, i.e. $\Delta = 1$, thus the full expression of our Green's function is

$$\begin{aligned} G(r, r') &= \frac{1}{2\pi |r - r' + (\Delta/\sqrt{2\pi})n|} \\ &= \frac{1}{2\pi \cdot \sqrt{(x-x')^2 + (y-y')^2 + z^2 + 1/\sqrt{2\pi}}} \end{aligned} \tag{44}$$

Now that the potential has been calculated for every point in our box, it is then used to calculate each of the three Cartesian components for the magnetic field at every point in the box which are also stored in three dimensional arrays. Recall that a potential/current-free field can be defined as the gradient of the potential scalar Φ. Thus we must include an algorithm in the program to calculate the derivative of the potential. One such method of calculating the derivative is the use of spectral methods. Although spectral methods are frequently used in numerical analysis, we choose to use a finite difference method to approximate the derivative. This has the advantage of faster computation times when running the program. We use the 4th order centred finite difference — the derivative of the function is computed from 4 values of the function (2 values on either side of the point where we want to calculate the derivative). The formula for this is given by[26]:

$$f'_i = \frac{(f_{i-2} - 8f_{i-1} + 8f_{i+1} - f_{i_2})}{12\delta x} \tag{45}$$

We see that the derivative for index/position `i` refers to the function at index `i-2`. This would lead to an index out of bounds error if our potential field box is the same size as that of the potential scalar. Thus to allow for these indices, we reduce the size of our box by two mesh points on each side, taking the potential scalar at the exterior regions as 'ghost cells'.

The 4th order finite difference algorithm computes the potential magnetic field component arrays which are then written to files with the `writeData` method and processed for plotting. The potential field data was visualised using VisIt, a tool developed by the United States Department of Energy. The data from the potential field files were compiled into the (legacy) Visualization Toolkit (VTK) file format in a python script using a .vtk file writer library (visit_writer.so) bundled with VisIt. The separate components of the potential field — B_x, B_y and B_z — can then be collated into the complete vector field and visualised using the VisIt tool.

4.2.2 *Results*

A region of 140×140 pixels was extracted from a HMI line-of-sight magnetogram taken on the 15th of January 2014. The centre of this region is located at $(2240, 1550)$. As mentioned earlier, the magnetogram images have a resolution of 4096 pixels on each side. There is roughly 20 pixels of empty space from the edges of the image to the edge of the sun so we can take the diameter of the sun to be approximately 4056 pixels. In more conventional SI units, the sun has a diameter of $D_{sun} = 1.39 \times 10^9 m$ therefore each pixel in the magnetogram represents $D_{sun}/4056 \approx 0.34 Mm$, thus our 140×140 pixel region is about $48 \times 48 Mm$. Figure 8 shows the magnetogram and the chosen region. Figure 9 shows a streamline plot of the extrapolated magnetic vector field, visualised using VisIt. Clear loop like structures are seen, bearing some resemblance to coronal loops. A comparison of the streamline plot with an extreme ultra violet (EUV) image taken from the AIA is shown in figure 10. The extrapolated coronal field has similar features to what is seen in the EUV image — both have a strong area of field lines extending from the centre of the left to the top of the box. However it is clear to see that the extrapolated potential field is a rather crude approximation of the coronal field when compared with the AIA image. In the constructed potential field model, field lines extend out through the right side of the box. This is not seen in the EUV image, in fact the field completely leaves the box through the top and does not touch the right edge.

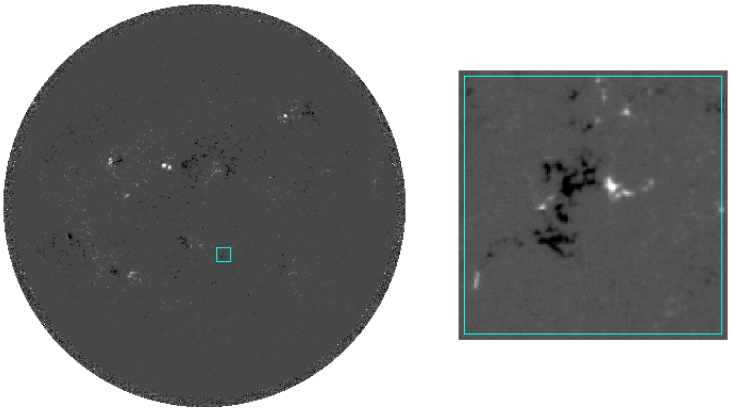

Figure 8: *Left*: Line of sight magnetogram from Helioseismic and Magnetic Imager taken on the 15th of January 2014. The 140×140 pixel region is shown within the cyan box.
Right: Enlarged image of the chosen region.

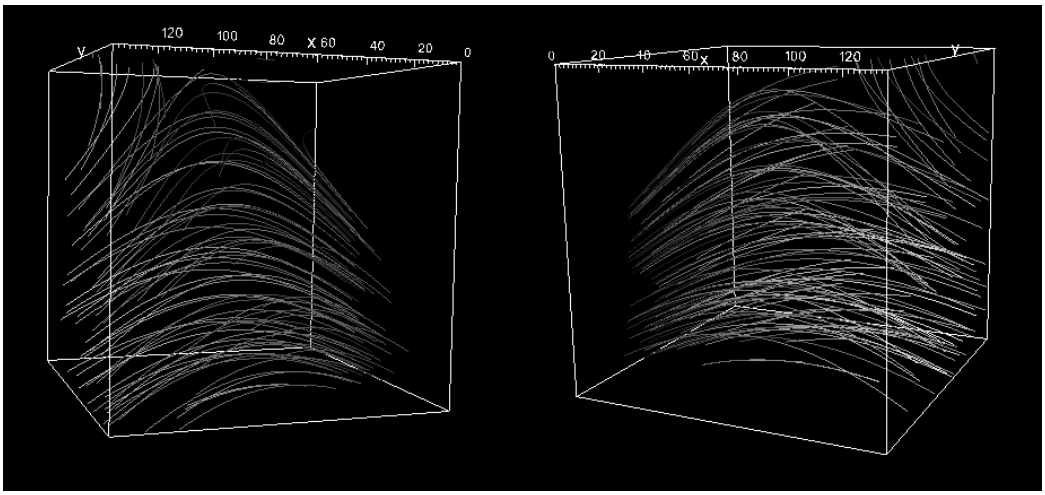

Figure 9: Streamline plots of the extrapolated potential magnetic field.

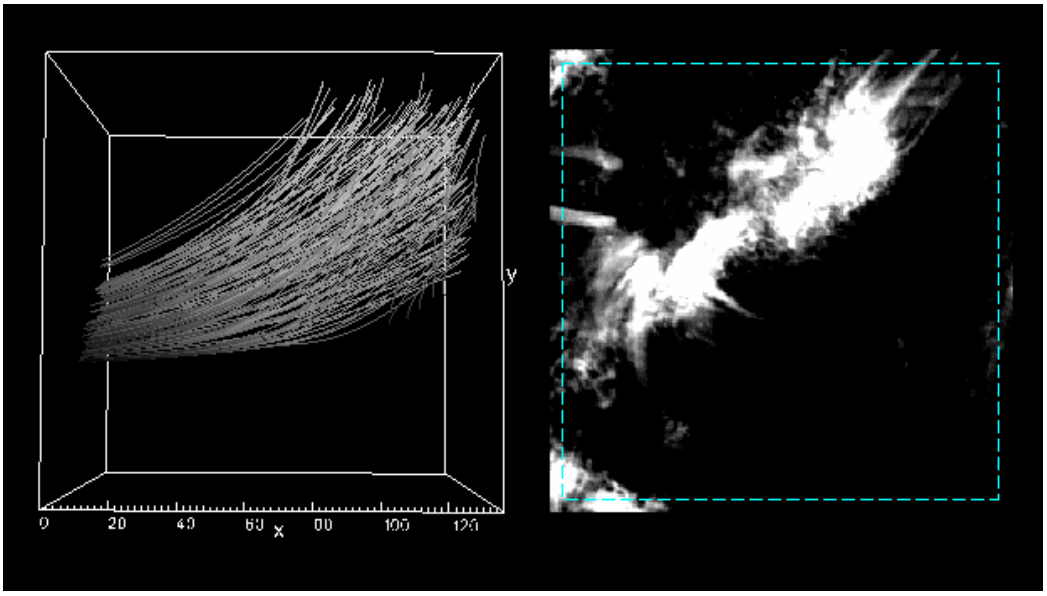

Figure 10: *Left*: Top down view of streamline plots of the extrapolated potential magnetic field. *Right*: Corresponding region from an Atmospheric Imaging Assembly image in the EUV wavelength range. Image shown was taken in the 171Åwavelength.

5

CONCLUSION

We have explored several methods of extrapolating the magnetic field of the solar corona from measurements of the photospheric field. This was seen to be necessary due to complications in observations. All models of the coronal magnetic field discussed were assumed to be force-free, that is to say all non-magnetic forces were negligible. Whilst this can be justified in the solar corona due to the low plasma β, the same cannot be said for the photosphere and chromosphere. However these models can serve as a good approximation, especially the non-linear force-free solutions. Our use of the Green's function method for potential field extrapolation was seen to produce similar results to EUV observations but unsuitable as an accurate representation. Since current models are constrained by assumptions which must be made due to observational limitations, it seems we must strive for improvements in our observational capabilities of magnetic fields in the corona. Nevertheless some progress has been made in recent decades in our understanding of the corona, especially the establishment of AC and DC heating models regarding coronal heating.

A

APPENDIX

A.1 MAIN PROGRAM

Normal magnetic field data file must be placed in directory named *input*. Potential field components are written to files in directory named *output*.

```
import java.io.BufferedReader;
import java.io.BufferedWriter;
import java.io.FileReader;
import java.io.FileWriter;
import java.util.ArrayList;
import java.util.Scanner;

public class Main {

        private static double twopi = Math.PI * 2;
        public static void main(String[] args) throws Exception {

                long startTime = System.currentTimeMillis();
                Scanner user_input = new Scanner(System.in);
                String filename;
                System.out.println("Enter file name for magnetic normal data: ");
                filename = user_input.next();
                System.out.print("Reading from file...");
                Double[][] data = readData(filename + ".csv");
                System.out.println(" Done!");

                //calculate potential scalar
                System.out.println("Running computations");
                double[][][] phi = new double[data.length][data.length][data.length];
                for (int X = 0; X < data.length; X++) {
                        for (int Y = 0; Y < data.length; Y++)
                                for (int Z = 0; Z < data.length; Z++)
                                        for (int Xd = 0; Xd < data.length; Xd++)
                                                for (int Yd = 0; Yd < data.length; Yd
                                                    ++) {
```

```
                                                    phi[X][Y][Z] += ((double)
                                                        data[Xd][Yd])*(1/twopi*
                                                        Math.sqrt((X - Xd)*(X -
                                                        Xd) + (Y - Yd)*(Y - Yd) +
                                                         (Z)*(Z) + (1/Math.sqrt(
                                                        twopi))));
                                        }
                System.out.println("..." + (data.length - 1 - X));
            }
            System.out.println("Done!");

            //calculate potential magnetic field components
            double[][][] Bx = new double[data.length - 4][data.length - 4][data.
                length - 4];
            double[][][] By = new double[data.length - 4][data.length - 4][data.
                length - 4];
            double[][][] Bz = new double[data.length - 4][data.length - 4][data.
                length - 4];
            for (int k = 2; k < data.length - 2; k++)
                for (int j = 2; j < data.length - 2; j++)
                    for (int i = 2; i < data.length - 2; i++) {
                        Bx[i-2][j-2][k-2] = (phi[i-2][j][k] - 8*phi[i
                            -1][j][k] + 8*phi[i+1][j][k] - phi[i+2][j
                            ][k])/12;
                        By[i-2][j-2][k-2] = (phi[i][j-2][k] - 8*phi[i
                            ][j-1][k] + 8*phi[i][j+1][k] - phi[i][j
                            +2][k])/12;
                        Bz[i-2][j-2][k-2] = (phi[i][j][k-2] - 8*phi[i
                            ][j][k-1] + 8*phi[i][j][k+1] - phi[i][j][
                            k+2])/12;
                    }
            //write vector components to file
            System.out.print("Writing to file.");
            writeData(Bx, "bx.dat");
            System.out.print(".");
            writeData(By, "by.dat");
            System.out.print(".");
            writeData(Bz, "bz.dat");
            System.out.println(" Done!");
```

```
56              long endTime = System.currentTimeMillis();

                long runTime = endTime - startTime;
                System.out.println("Run time: " + runTime/1000.0 + " seconds");

61      }

        public static Double[][] readData(String filename) throws Exception {

                ArrayList<String> rawData = new ArrayList<>();
66              BufferedReader reader = new BufferedReader(new FileReader("input/" +
                    filename));

                String line;
                while ((line = reader.readLine()) != null) rawData.add(line);
                reader.close();
71
                String[] output = new String[rawData.size()];
                return parseData(rawData.toArray(output));

        }
76
        public static Double[][] parseData(String[] rawData) {

                ArrayList<Double[]> parsedData = new ArrayList<>();
                for (int i = 0; i < rawData.length; i++) {
81                      String[] temp = rawData[i].split(",");

                        Double[] row = new Double[temp.length];
                        for (int j = 0; j < temp.length; j++) row[j] = Double.
                            parseDouble(temp[j].replace("\"", ""));

86                      parsedData.add(row);
                }

                Double[][] output = new Double[parsedData.size()][parsedData.get(0).
                    length];
                return  parsedData.toArray(output);
91
        }
```

```
        public static void writeData(double[][][] data, String filename) throws
            Exception {

                BufferedWriter writer = new BufferedWriter(new FileWriter("output/" +
                     filename));

                for (int x = 0; x < data.length; x++)
                        for (int y = 0; y < data[x].length; y++)
                                for (int z = 0; z < data[x][y].length; z++)
                                        writer.write(Double.toString(data[x][y][z]) +
                                             "\n");
                writer.close();

        }

}
```

A.2 COMPILER TO .VTK FORMAT FOR VISUALIZATION

This must be placed in the *output* directory.

```
import visit_writer, math

#open files for reading
f = open('bx.dat', 'r')
g = open('by.dat', 'r')
h = open('bz.dat', 'r')
points = int(raw_input('How many pixels on side of region chosen?'))-3
#setup dimensions
NX = points
NY = points
NZ = points
#read data to temporary arrays
vecx = []
vecy = []
vecz = []
for line in h:
        vecz.append(float(line.strip()))
```

```
for line in g:
        vecy.append(float(line.strip()))
for line in f:
        vecx.append(float(line.strip()))

#create nodal variable for x component of mag field
index = 0
magxcomp = []
for k in range(NZ):
        for j in range(NY):
                for i in range(NX):
                        magxcomp.append(vecx[index])
                        index += 1
#create nodal variable for y component of mag field
index = 0
magycomp = []
for k in range(NZ):
        for j in range(NY):
                for i in range(NX):
                        magycomp.append(vecy[index])
                        index += 1
#create nodal variable for z component of mag field
magzcomp = []
index = 0
for k in range(NZ):
        for j in range(NY):
                for i in range(NX):
                        magzcomp.append(vecz[index])
                        index = index + 1
dims = (NX, NY, NZ)
vars = (("magxcomp", 1, 1, magxcomp), ("magycomp", 1, 1, magycomp), ("magzcomp", 1,
    1, magzcomp))
visit_writer.WriteRegularMesh("plottabledata.vtk", 0, dims, vars)
```

BIBLIOGRAPHY

[1] Tsiklauri, D. *Missing pieces of the solar jigsaw puzzle*. Astronomy & Geophysics 2009; **50**(5):5.32-5.38.

[2] Backman, D.; Seeds, M. *The Solar System*. Seventh Edition. Cengage. 2011.

[3] Aschwanden, M.J.; Winebarger, A.; Tsiklauri, D.; Peter, H. *The Coronal Heating Paradox*. The Astrophysical Journal 2007; **659**(2):1673-1681.

[4] Parker, E.N. *Nanoflares and the solar X-ray corona*. Astrophysical Journal 1988; **330**:474-479.

[5] Klimchuk, A.J. *Solving the Coronal Heating Problem*. Solar Physics 2006; **234**(1):41-77.

[6] Iwai, K.; Shinya, K.; Takashi, K.; Moreau, R. *Pressure change accompanying Alfvén waves in a liquid metal*. Magnetohydrodynamics 2003; **39**(3):245-250.

[7] Alfven, H. *Existence of Electromagnetic-Hydrodynamic Waves*. Nature 1942; **150**(3805):405-406.

[8] Benz, A.O. *Flare Observations*. Living Reviews in Solar Physics 2008;**5**(1).

[9] Bowness, R.; Hood, A. W.; Parnell, C. E. *Coronal heating and nanoflares: current sheet formation and heating*. Astronomy & Astrophysics 2013; **560**(A89):14.

[10] Vainshtein, S.I. *Anomalous resistivity as the possible cause of fast reconnection in the solar corona*. Solar Physics 1989; **124**(1):129-144.

[11] Vaiana, G.S. and Rosner, R. *Recent Advances in Coronal Physics*. Annual Review of Astronomy and Astrophysics 1978; **16**:393-428.

[12] Altschuler, M. D. *Magnetic Structure Responsible for Coronal Disturbances: Observations*. Coronal Disturbances 1974; proceedings from IAU Symposium 57.

[13] Poletto, G.; Vaiana G.S.; Zombeck M.V.; Krieger A.S. and Timothy A.F. *A comparison of coronal X-ray structures of active regions with magnetic fields computed from photospheric observations*. Solar Physics 1975; **44**:83-99.

[14] Aschwanden, M. *Physics of the Solar Corona*. First Edition. Springer. 2005.

[15] Schmidt, H.U. *On the Observable Effects of Magnetic Energy Storage and Release Connected With Solar Flares*. NASA Special Publication 1964; **50**:107.

[16] Sakurai, T. *Green's Function Methods for Potential Magnetic Fields*. Solar Physics 1982; **76**(2):301-321.

[17] Metcalf, T.R.; DeRosa, M.K.; Schrijver, C.J.; Liu, Y.; McTiernan, J.; Regnier, S. et al. *Nonlinear Force-Free Modeling of Coronal Magnetic Fields Part I: A Quantitative Comparison of Methods*. Solar Physics 2006; **235**(1-2):161-190.

[18] Metcalf, T.R.; DeRosa, M.L.; Schrijver, C.J.; Barnes G.; van Ballegooijen, A.A.; Wiegelmann T. et al. *Nonlinear Force-Free Modeling of Coronal Magnetic Fields. II. Modeling a Filament Arcade and Simulated Chromospheric and Photospheric Vector Fields* Solar Physics 2008; **247**(2):269-299.

[19] Seehafer, N. *Determination of constant alpha force-free solar magnetic fields from magnetograph data*. Solar Physics 1978; **58**:215-223.

[20] Chiu, Y. T. and Hilton, H. H. *Exact Green's function method of solar force-free magnetic-field computations with constant alpha. I - Theory and basic test cases*. Astrophysical Journal, Part 1 1977; **212**:873-885.

[21] Alissandrakis, C. E. *On the computation of constant alpha force-free magnetic field*. Astronomy and Astrophysics 1981; **100**(1):197-200.

[22] Wiegelmann, T. *Nonlinear force-free modeling of the solar coronal magnetic field*. Journal of Geophysical Research (Space Physics) 2008; **113**(A3).

[23] Wiegelmann, T. *Optimization code with weighting function for the reconstruction of coronal magnetic fields*. Solar Physics 2004; **219**(1):87-108.

[24] Abhyankar, K.D. *A Survey of the Solar Atmospheric Models*. Bulletin of the Astronomical Society of India 1977; **5**:40.

[25] Jackson, J.D. *Classical Electrodynamics*. Third Edition. John Wileys & Sons, Inc. 1925.

[26] Brandenburg, A. *Computational aspects of astrophysical MHD and turbulence*. Advances in Nonlinear Dynamics. Taylor and Francis Group. 2003

[27] Sakurai, T. *Calculation of force-free magnetic field with non-constant alpha* Solar Physics 1981; **69**(2):343-359.

[28] Zhu, X.S.; Wang, H.N.; Du, Z.L.; Fan, Y.L. *Forced Field Extrapolation: Testing a Magnetohydrodynamic (MHD) Relaxation Method with a Flux-rope Emergence Model*. The Astrophysical Journal 2013; **768**(2):7.